Molecular-dynamics approach to itinerant magnetism with complex magnetic structures. II. Site-dependent medium and its application to γ-Mn

Y. Kakehashi, H. Al-Attar, and N. Kimura
Hokkaido Institute of Technology, Maeda, Teine-ku, Sapporo 006, Japan
(Received 27 October 1998)

A molecular-dynamics (MD) theory of itinerant magnetism with complex magnetic structure has been improved by introducing a site-dependent noncollinear effective medium. It takes into account the molecular fields from distant local magnetic moments in a self-consistent way, therefore, allowing us to describe reasonably the temperature dependence of magnetic moments showing complex structures. The theory is applied to γ-Mn with 108 atoms in a MD unit cell. It is demonstrated that the MD approach with the site-dependent medium can describe the second-order phase transition with increasing temperature. Calculated Néel temperature (T_N) is shown to be comparable to the experimental value. It is found that the magnetic short-range orders at T_N are rather small, but the 1st and 3rd nearest-neighbor short-range orders show very weak temperature dependence above T_N. The calculated densities of states show a strong temperature dependence below T_N and the peak near the top of the *d* bands is shown to remain even above T_N. [S0163-1829(99)04913-9]

I. INTRODUCTION

Itinerant-electron systems with competing magnetic interactions often show the complex magnetic structures, which interrupt the understanding of their magnetic properties.[1–5] The determination of these structures has been a basic subject in both experiment and theory.[6] The past theories for the magnetic structures of itinerant-electron systems relied on a simple energy comparison among possible magnetic structures,[7,8] energy minimization with respect to the order parameters obtained by experiments,[9–11] or the susceptibility analysis for the magnetic instability.[12] These methods, however, do not guarantee theoretically that the obtained structure yields the lowest energy of the systems. One needs to establish a more solid theory to determine the magnetic structure in itinerant-electron systems.

We proposed in the previous paper[13] (which is referred to as I hereafter) a molecular-dynamics (MD) approach to the complex magnetic structures of itinerant-electron systems on the basis of the functional integral method[14–16] and isothermal MD technique.[17,18] In this approach, we directly calculate the thermal average by means of the time average of the fictitious spins assuming the ergodicity of the system. The magnetic forces in the equations of motion are calculated from the Green function of the electron systems in which the outside of the MD unit cell for each atom is described by a uniform effective medium. The method allows us to determine automatically the magnetic structure of the system with a large number of atoms N in a unit cell at finite temperatures.

We applied in I the approach to the fcc transition metals with use of 108 atoms (i.e., $3\times3\times3$ fcc lattice), and found various complex magnetic structures for *d* electron numbers between 6.0 and 7.0. In the following paper,[19] we extended the theory to magnetic alloys, and explained with use of $N=108$ atoms the complex magnetic structures of γFe-Mn alloys from the first-kind antiferromagnetic (AF) structure to noncollinear complex structures with the change of concentration. In particular, the concentration dependence of average magnetic moments showing a peculiar minimum at 50 at. % Fe was explained by means of the MD approach.

The calculations of the temperature dependence of magnetic moments based on the MD approach, on the other hand, have been done so far only for α-Fe with use of $N=128$ atoms and uniform polarized medium. We reported in I that the second-order magnetic transition with a reasonable Curie temperature 950 K is obtained for α-Fe when the medium is self-consistently determined. We recently extended the same calculations to γ-Mn with the use of $N=108$ atoms. The MD approach, however, yielded the first-order transition to the paramagnetic state around 150 K, which is not consistent with the experimental data. Although the problem should be removed in principle with increasing the number of atoms N in the simulations, the recent MD calculations with use of classical Heisenberg model by Antropov, Tretyakov, and Harmon[20] reveals that the nature of transition hardly changes even if the size is increased from $N=512$ to $N=3375$. Since the number of atoms in the present MD calculations is limited to several hundred in maximum at the present stage, one needs to develop further the theory of MD for rather small number of atoms N to describe the second-order transition of magnetic moments with complex magnetic structure.

In this paper, we improve the MD approach presented in I, introducing a site-dependent noncollinear effective medium, which describes the magnetic forces from the distant magnetic moments more accurately. Applying the improved theory to γ-Mn, we will demonstrate that the theory can describe the second-order phase transition in the systems having complex magnetic structures with increasing temperature.

In the next section, we summarize the outline of the MD approach in I. Next, we introduce the site-dependent noncollinear effective medium to take into account the static magnetic interactions between distant local magnetic moments in the ordered state. Expanding the site-dependent medium

from the paramagnetic state, we derive a simplified expression being suitable for the MD calculations. In Sec. III, we present the numerical results of calculations for γ-Mn obtained by the improved MD approach: the magnetic moments vs temperature curves, the magnetic short-range orders (MSRO) vs temperature curves, and the temperature dependence of densities of states (DOS). We will demonstrate that the improved MD yields the second-order phase transition from the first-kind AF to the paramagnetic state with increasing temperatures. Comparing the calculated MSRO's of γ-Mn with those of α-Fe, we will show that the spin frustrations can suppress the temperature dependence of the MSRO's and furthermore that the DOS in the paramagnetic state is quite different from those in the coherent potential approximation (CPA). In the last section, we summarize the MD approach and the results of calculation for γ-Mn at finite temperatures.

II. MD APPROACH WITH SITE-DEPENDENT MEDIUM

A. MD approach

We briefly review the MD approach presented in I in this subsection. We start from the tight-binding Hamiltonian as

$$H=H_0+H_1, \tag{1}$$

$$H_0=\sum_{i\nu\sigma}\epsilon_i^0 n_{i\nu\sigma}+\sum_{i\nu j\nu'\sigma}t_{i\nu j\nu'}a_{i\nu\sigma}^{\dagger}a_{j\nu'\sigma}, \tag{2}$$

$$H_1=\frac{1}{4}\sum_i U_i\hat{n}_i^2-\sum_i J_i\hat{\mathbf{S}}_i^2. \tag{3}$$

Here, ϵ_i^0 and $t_{i\nu j\nu'}$ are the atomic level on site i and the transfer integral between the orbitals ν on site i and ν' on site j, respectively. $U_i(J_i)$ denotes the intraatomic Coulomb (exchange) integrals on site i. $a_{i\nu\sigma}^{\dagger}(a_{i\nu\sigma})$ is the creation (annihilation) operator for an electron with spin σ and orbital ν on site i. Moreover, $n_{i\nu\sigma}=a_{i\nu\sigma}^{\dagger}a_{i\nu\sigma}$ is the number operator for the electrons on site i, orbital ν, and spin σ. $\hat{n}_i$ and $\hat{\mathbf{S}}_i$ in the interaction part H_1 denote the charge and spin densities on site i, which are defined by $\hat{n}_i=\Sigma_{\nu\sigma}n_{i\nu\sigma}$ and $\hat{\mathbf{S}}_i=\Sigma_{\nu\sigma\sigma'}a_{i\nu\sigma}^{\dagger}(\boldsymbol{\sigma})_{\sigma\sigma'}a_{i\nu\sigma'}/2$, respectively, $\boldsymbol{\sigma}$ being the Pauli spin matrices.

We adopt the functional integral method to the above Hamiltonian written on the locally rotated coordinates, and make the static approximation, which reduces to the generalized Hartree-Fock approximation at the ground state. The local magnetic moment (LM) on site i is then written by using the field variables $\{\boldsymbol{\xi}_i\}$ acting on each site as follows.

$$\langle\mathbf{m}_i\rangle=\frac{\int\left[\prod_j d\boldsymbol{\xi}_j\right]\left(1+\frac{4}{\beta\tilde{J}_i\xi_i^2}\right)\boldsymbol{\xi}_i e^{-\beta\Psi(\boldsymbol{\xi})}}{\int\left[\prod_j d\boldsymbol{\xi}_j\right]e^{-\beta\Psi(\boldsymbol{\xi})}}, \tag{4}$$

$$\Psi(\boldsymbol{\xi})=-\beta^{-1}\ln\mathrm{Tr}(e^{-\beta H_{st}(\boldsymbol{\xi})})-\sum_i\left[n_i w_i(\boldsymbol{\xi})-\frac{1}{4}\tilde{J}_i\xi_i^2\right]+2T\sum_i\ln\xi_i, \tag{5}$$

$$H_{st}(\boldsymbol{\xi})=\sum_{i\nu\sigma}[\epsilon_i^0-\mu+w_i(\boldsymbol{\xi})]n_{i\nu\sigma}-\frac{1}{2}\sum_i\tilde{J}_i\boldsymbol{\xi}_i\cdot\mathbf{m}_i+\sum_{i\nu j\nu'\sigma}t_{i\nu j\nu'}a_{i\nu\sigma}^{\dagger}a_{j\nu'\sigma}. \tag{6}$$

Here, $m_{i\nu\alpha}=\Sigma_{\sigma\sigma'}a_{i\nu\sigma}^{\dagger}(\sigma_\alpha)_{\sigma\sigma'}a_{i\nu\sigma'}$. β denotes the inverse temperature T^{-1}, and μ is the chemical potential. The effective exchange parameter $\tilde{J}_i$ is defined by $\tilde{J}_i=U_i/2D+(1+1/2D)J_i$, D being the number of orbital degeneracy. n_i is the electron number satisfying the charge neutrality on site i. The charge potential $w_i(\boldsymbol{\xi})$ is determined by the charge neutrality condition on each site:

$$n_i=\int d\omega f(\omega)\frac{(-)}{\pi}\mathrm{Im}\sum_{\nu\sigma}G_{i\nu\sigma}(\omega+i\delta,\boldsymbol{\xi}), \tag{7}$$

$$G_{i\nu\sigma}(z,\boldsymbol{\xi})=(G)_{i\nu\sigma i\nu\sigma}=\{[z-H_{st}(\boldsymbol{\xi})]^{-1}\}_{i\nu\sigma i\nu\sigma}. \tag{8}$$

Here, $f(\omega)$ is the Fermi-distribution function, $G_{i\nu\sigma}$ is the diagonal Green function for the one-electron Hamiltonian $H_{st}(\boldsymbol{\xi})$, and $z=\omega+i\delta$, δ being an infinitesimal positive number.

In the MD approach, we regard $\Psi(\boldsymbol{\xi})$ as a classical potential to the variables $\{\boldsymbol{\xi}_i(t)\}$, and calculate the thermal average (4) by means of the time average as follows.

$$\langle\mathbf{m}_i\rangle=\lim_{t_0\to\infty}\frac{1}{t_0}\int_0^{t_0}\left[1+\frac{4}{\beta\tilde{J}_i\xi_i^2(t)}\right]\boldsymbol{\xi}_i(t)dt. \tag{9}$$

We adopt the isothermal MD equations of motion[17] for the time development of the variables $\{\boldsymbol{\xi}_i(t)\}$.

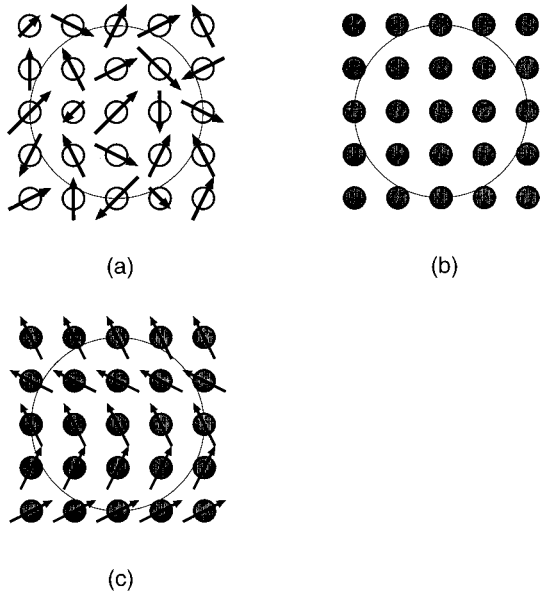

FIG. 1. Schematic representations for the system having time-dependent fictitious local moments (LM) $\{\xi_i(t)\}$ (a), a coherent system with uniform medium (b), and the system with site-dependent noncollinear medium (c). The large circle drawn by thin curve shows a cluster corresponding to the maximum recursion level for the central site.

$$\dot{\xi}_{i\alpha}=\frac{p_{i\alpha}}{\mu_{\mathrm{LM}}}, \tag{10}$$

$$\dot{p}_{i\alpha}=\frac{1}{2}\tilde{J}_i(\langle m_{i\alpha}\rangle_0-\xi_{i\alpha})-\frac{2T\xi_{i\alpha}}{\xi_i^2}-\zeta_\alpha p_{i\alpha}, \tag{11}$$

$$\dot{\zeta}_\alpha=\frac{1}{Q}\left(\sum_i \frac{p_{i\alpha}^2}{\mu_{\mathrm{LM}}}-NT\right). \tag{12}$$

Here, μ_{LM} is the effective mass for the LM on site i and Q in Eq. (12) denotes a constant parameter. $p_{i\alpha}$ is the fictitious momentum conjugate to the exchange field $\xi_{i\alpha}$. The first and second terms at the rhs (right-hand side) of Eq. (11) are a magnetic force, and the third term is the friction force describing the heat-bath effects, which is controlled by changing the coefficient ζ_α according to Eq. (12).

It should be noted that all the electronic structures enter into the magnetic force in Eq. (11) via the time-dependent local magnetization defined by

$$\langle \mathbf{m}_i\rangle_0=\int d\omega f(\omega)\frac{(-)}{\pi}\mathrm{Im}\sum_{\nu\sigma}(\boldsymbol{\sigma}G)_{i\nu\sigma i\nu\sigma}. \tag{13}$$

B. Site-dependent effective medium

According to Eq. (13), we need to calculate the diagonal Green function $G_{i\nu\alpha}=(G)_{i\nu\alpha i\nu\alpha}$ at each step in the MD approach. Here, $\{|i\nu\alpha\rangle\}$ denote a basis set that diagonalizes the Pauli spin matrices. Since the charge and exchange potentials can change at random in both space and time [see Fig. 1(a)], we adopt the recursion method[21–23] for the calculation of the Green function at each time step.

$$G_{i\nu\alpha}(z,\boldsymbol{\xi})=\cfrac{1}{z-a_{1i\nu\alpha}(\boldsymbol{\xi})-\cfrac{|b_{1i\nu\alpha}(\boldsymbol{\xi})|^2}{z-a_{2i\nu\alpha}(\boldsymbol{\xi})-\cfrac{|b_{2i\nu\alpha}(\boldsymbol{\xi})|^2}{\cdots\cfrac{}{\cdots-\cfrac{|b_{l-1i\nu\alpha}(\boldsymbol{\xi})|^2}{z-a_{li\nu\alpha}(\boldsymbol{\xi})-T_{li\nu\alpha}(z,\boldsymbol{\xi})}}}}}. \tag{14}$$

Here, $a_{li\nu\alpha}(\boldsymbol{\xi})$ and $b_{li\nu\alpha}(\boldsymbol{\xi})$ are the recursion coefficients of the lth order. $T_{li\nu\alpha}(z,\boldsymbol{\xi})$ is the terminator at the lth level.

In the previous theory, we considered a unit cell with N atoms for the MD calculations, and obtained the Green functions in Eq. (13) from the formula (14). The level l for the terminator was taken to be the maximum value such that the terminator does not cause any artificial interactions due to the periodic boundary condition. The terminator $T_{li\nu\alpha}(z,\boldsymbol{\xi})$ was then approximated by the terminator $\mathcal{T}_{l\nu\alpha}(z)$ for the coherent Green function with uniform medium [see Fig. 1(b)].

$$F_{i\nu\alpha i\nu\alpha}=[(\mathcal{L}^{-1}-t)^{-1}]_{i\nu\alpha i\nu\alpha}. \tag{15}$$

Here, $[\mathcal{L}^{-1}(z)]_{i\nu\sigma j\nu'\sigma'}=\mathcal{L}_\sigma^{-1}(z)\delta_{ij}\delta_{\nu\nu'}\delta_{\sigma\sigma'}$ is a uniform effective medium and $(t)_{i\nu\sigma j\nu'\sigma'}=t_{ij\nu\nu'}\delta_{\sigma\sigma'}$. In this approximation, the effect of the long-range order is not taken into account in the medium except the case of ferromagnetism.

In the present paper, we introduce the site-dependent noncollinear effective medium

$$[\mathcal{L}^{-1}(z)]_{i\nu\sigma j\nu'\sigma'}=[\mathcal{L}_i^{-1}(z)]_{\sigma\sigma'}\delta_{ij}\delta_{\nu\nu'}, \tag{16}$$

and approximate the terminator by that of the site-dependent coherent Green function (15) in which the medium has been replaced by Eq. (16).

$$T_{li\nu\alpha}(z,\boldsymbol{\xi})\approx\mathcal{T}_{li\nu\alpha}(z). \tag{17}$$

The site-dependent effective medium $\mathcal{L}_i^{-1}$ can be determined by the local CPA (coherent potential approximation) condition[24] at each site.

$$\langle G_i\rangle=F_i. \tag{18}$$

Here, $\langle\sim\rangle$ denotes the thermal average with respect to the energy (5), G_i is the impurity Green function defined by

$$G_i=(L_i^{-1}-\mathcal{L}_i^{-1}+F_i^{-1})^{-1}, \tag{19}$$

$$(L_i^{-1})_{\nu\sigma\nu'\sigma'}=[z-\epsilon_i^0+\mu-w_i(\boldsymbol{\xi})]\delta_{\nu\nu'}\delta_{\sigma\sigma'}+\frac{1}{2}\tilde{J}_i\boldsymbol{\xi}_i\cdot(\boldsymbol{\sigma})_{\sigma\sigma'}\delta_{\nu\nu'}, \tag{20}$$

$$(F_i)_{\nu\sigma\nu'\sigma'}=[(\mathcal{L}^{-1}-t)^{-1}]_{i\nu\sigma i\nu'\sigma'}. \tag{21}$$

To simplify the electronic structure calculations, we expand the site-dependent effective medium $\mathcal{L}_i^{-1}$ from the uniform medium $\tilde{\mathcal{L}}^{-1}$ in the paramagnetic state.

$$\mathcal{L}_i^{-1}=\tilde{\mathcal{L}}^{-1}+\delta\mathcal{L}_i^{-1}. \tag{22}$$

The uniform medium $\tilde{\mathcal{L}}^{-1}$ is determined by the CPA equation in the paramagnetic state.

$$\langle\tilde{G}_i\rangle_0=\tilde{F}. \tag{23}$$

Here, $\langle\sim\rangle_0$ denotes the thermal average in a paramagnetic state, and $\tilde{G}_i$ and $\tilde{F}$ are defined by Eqs. (19) and (21) in which $\mathcal{L}_i^{-1}$ has been replaced by $\tilde{\mathcal{L}}^{-1}$.

Substituting Eq. (22) into Eq. (18) and linearizing the equation with respect to $\delta\mathcal{L}_i^{-1}$, we obtain

$$\tilde{F}\delta\mathcal{L}_i^{-1}\tilde{F}+\sum_{j\neq i}\tilde{F}_{ij}\delta\mathcal{L}_j^{-1}\tilde{F}_{ji} -\left\langle \tilde{G}_i\tilde{F}^{-1}\sum_{j\neq i}\tilde{F}_{ij}\delta\mathcal{L}_j^{-1}\tilde{F}_{ji}\tilde{F}^{-1}\tilde{G}_i\right\rangle=\tilde{F}-\langle\tilde{G}_i\rangle. \tag{24}$$

Making use of the decoupling approximation to the thermal average $\langle\sim\rangle$ and use of the CPA Eq. (23) at the lhs of the above equation, we obtain

$$\delta\mathcal{L}_i^{-1}=\tilde{F}^{-1}-\tilde{F}^{-1}\langle\tilde{G}_i\rangle\tilde{F}^{-1}. \tag{25}$$

We assume that the medium $\delta\mathcal{L}_i^{-1}$ is polarized in a direction of $\mathbf{e}_i=\langle\boldsymbol{\xi}_i\rangle/|\langle\boldsymbol{\xi}_i\rangle|$. It is then diagonalized along $\mathbf{e}_i$ axis. Therefore, Eq. (25) is written by using the spin states σ, which diagonalize $\sigma_z'=\mathbf{e}_i\cdot\boldsymbol{\sigma}$ as follows:

$$\delta\mathcal{L}_{i\Gamma\sigma}^{-1}=\tilde{F}_\Gamma^{-1}-\tilde{F}_\Gamma^{-1}\langle\tilde{G}_{i\Gamma\sigma}\rangle\tilde{F}_\Gamma^{-1}. \tag{26}$$

We assumed in Eq. (26) that all the sites are equivalent in the paramagnetic state, and Γ denotes the irreducible representation of a point symmetry of the crystal. The coherent Green function in the paramagnetic state in Eq. (26) is expressed as

$$\tilde{F}_\Gamma=\int\frac{\rho_\Gamma(\epsilon)d\epsilon}{\tilde{\mathcal{L}}_\Gamma^{-1}-\epsilon}. \tag{27}$$

Here, $\rho_\Gamma(\epsilon)$ is the DOS for the transfer matrix $t_{i\nu j\nu'}$, which is projected onto one of the orbitals belonging to the representation Γ.

The Green function $\tilde{G}_{i\Gamma\sigma}$ in Eq. (26) is expressed as follows:

$$\tilde{G}_{i\Gamma\sigma}(z,\xi_{iz}',\xi_{i\perp}'^2)=\frac{L_{i-\sigma}^{-1}(z,\xi_{iz}',\xi_{i\perp}'^2)-\tilde{\mathcal{L}}_\Gamma^{-1}+\tilde{F}_\Gamma^{-1}}{\det_{i\Gamma}(z,\xi_{iz}',\xi_{i\perp}'^2)}, \tag{28}$$

$$L_{i\sigma}^{-1}(z,\xi_{iz}',\xi_{i\perp}'^2)=z-\epsilon_0+\mu-w_i(\boldsymbol{\xi})+\tfrac{1}{2}\tilde{J}\xi_{iz}'\sigma, \tag{29}$$

$$\det_{i\Gamma}(z,\xi_{iz}',\xi_{i\perp}'^2)=(L_{i\uparrow}^{-1}-\tilde{\mathcal{L}}_\Gamma^{-1}+\tilde{F}_\Gamma^{-1})(L_{i\downarrow}^{-1}-\tilde{\mathcal{L}}_\Gamma^{-1}+\tilde{F}_\Gamma^{-1}) -\tfrac{1}{4}\tilde{J}_i^2\xi_\perp'^2. \tag{30}$$

Here, $\xi_{iz}'=\mathbf{e}_i\cdot\boldsymbol{\xi}_i$ and $\xi_{i\perp}'=|(\mathbf{e}_i\times\boldsymbol{\xi}_i)\times\mathbf{e}_i|$.

Making use of the decoupling approximation, which is correct up to the second order, the average Green function in Eq. (26) is written as

$$\langle\tilde{G}_{i\Gamma\sigma}\rangle=\sum_{\lambda=\pm1}\frac{1}{2}\left(1+\lambda\frac{\langle\xi_{iz}'\rangle}{\langle\xi_{iz}'^2\rangle^{1/2}}\right)\tilde{G}_{i\Gamma\sigma}(z,\lambda\langle\xi_{iz}'^2\rangle^{1/2},\langle\xi_{i\perp}'^2\rangle). \tag{31}$$

Moreover, we replace $\langle\xi_{iz}'^2\rangle$ and $\langle\xi_{i\perp}'^2\rangle$ with $\langle\xi_{iz}'^2\rangle_0$ and $\langle\xi_{i\perp}'^2\rangle_0$ in the above equation since the differences should be of order of $(\delta\mathcal{L}_i^{-1})^2$.

Substituting Eq. (31) into Eq. (26) and using the CPA Eq. (23) in which the decoupling approximation (31) has been made, we obtain

$$\delta\mathcal{L}_{i\Gamma\sigma}^{-1}=\tfrac{1}{2}\tilde{J}_i\langle\xi_{iz}'\rangle\sigma[1+(\overline{L_i}^{-1}-\tilde{\mathcal{L}}_\Gamma^{-1})\tilde{F}_\Gamma]^{-1}, \tag{32}$$

where

$$\overline{L_i}^{-1}=z-\epsilon_0+\mu-w_i(\langle\xi_{iz}'^2\rangle^{1/2},\langle\xi_{i\perp}'^2\rangle). \tag{33}$$

Equation (32) means that

$$\delta\mathcal{L}_{i\Gamma}^{-1}=\tfrac{1}{2}\tilde{J}_i\langle\boldsymbol{\xi}_i\rangle\cdot\boldsymbol{\sigma}\,[1+(\overline{L_i}^{-1}-\tilde{\mathcal{L}}_\Gamma^{-1})\tilde{F}_\Gamma]^{-1}. \tag{34}$$

Neglecting the energy dependence in $\delta\mathcal{L}_{i\Gamma}^{-1}$ as well as the orbital dependence in the uniform medium, we obtain the final expression of the site-dependent effective medium as

$$\mathcal{L}_i^{-1}=\mathcal{L}_p^{-1}+\tfrac{1}{2}\tilde{J}_i\langle\boldsymbol{\xi}_i\rangle\cdot\boldsymbol{\sigma}. \tag{35}$$

We determine the uniform medium $\mathcal{L}_p^{-1}$ in the above equation by means of the averaged CPA equation.

$$\sum_\Gamma\frac{d_\Gamma}{D}\sum_{\lambda=\pm1}\frac{1}{2}\tilde{G}_{\Gamma\sigma}(z,\lambda\{[\langle\xi^2\rangle]_{\mathrm{av}}/3\}^{1/2},\{2[\langle\xi^2\rangle]_{\mathrm{av}}/3\}^{1/2}) =\sum_\Gamma\frac{d_\Gamma}{D}\tilde{F}_\Gamma. \tag{36}$$

Here, we omitted the site indices. d_Γ is the number of orbitals belonging to the irreducible representation Γ, $[\,]_{\mathrm{av}}$ denotes the average over sites, and $\tilde{F}_\Gamma$ is defined by Eq. (27) in which $\tilde{\mathcal{L}}_\Gamma^{-1}$ has been replaced by $\mathcal{L}_p^{-1}$.

Substituting Eq. (35) into Eq. (15) and using the recursion method, we obtain the site-dependent coherent Green function as

$$F_{i\nu\alpha i\nu\alpha}=\cfrac{1}{\mathcal{L}_p^{-1}-\tilde{a}_{1i\nu\alpha}(\langle\boldsymbol{\xi}\rangle)-\cfrac{|\tilde{b}_{1i\nu\alpha}(\langle\boldsymbol{\xi}\rangle)|^2}{\mathcal{L}_p^{-1}-\tilde{a}_{2i\nu\alpha}(\langle\boldsymbol{\xi}\rangle)-\cfrac{|\tilde{b}_{2i\nu\alpha}(\langle\boldsymbol{\xi}\rangle)|^2}{\cdots\;\cdots-\cfrac{|\tilde{b}_{l-1i\nu\alpha}(\langle\boldsymbol{\xi}\rangle)|^2}{\mathcal{L}_p^{-1}-\tilde{a}_{li\nu\alpha}(\langle\boldsymbol{\xi}\rangle)-\mathcal{T}_{li\nu\alpha}(\langle\boldsymbol{\xi}\rangle)}}}}. \tag{37}$$

Here, $\tilde{a}_{li\nu\alpha}(\langle\boldsymbol{\xi}\rangle)$ and $\tilde{b}_{li\nu\alpha}(\langle\boldsymbol{\xi}\rangle)$ are the recursion coefficients for the Hamiltonian $(\tilde{J}_i\langle\boldsymbol{\xi}_i\rangle\cdot\boldsymbol{\sigma}/2)\,\delta_{ij}\delta_{\nu\nu'}+t_{i\nu j\nu'}\delta_{\sigma\sigma'}$.

The terminator $\mathcal{T}_{li\nu\alpha}$ is obtained by considering larger cluster and using the recursive formula as follows:

$$\mathcal{T}_{li\nu\alpha}(\langle\boldsymbol{\xi}\rangle)=\cfrac{|\tilde{b}_{li\nu\alpha}(\langle\boldsymbol{\xi}\rangle)|^2}{\mathcal{L}_p^{-1}-\tilde{a}_{l+1i\nu\alpha}(\langle\boldsymbol{\xi}\rangle)-\cfrac{|\tilde{b}_{l+1i\nu\alpha}(\langle\boldsymbol{\xi}\rangle)|^2}{\cdots\cfrac{}{\cdots-\cfrac{|\tilde{b}_{m-1i\nu\alpha}(\langle\boldsymbol{\xi}\rangle)|^2}{\mathcal{L}_p^{-1}-\tilde{a}_{mi\nu\alpha}(\langle\boldsymbol{\xi}\rangle)-\mathcal{T}_{mi\nu\alpha}(\langle\boldsymbol{\xi}\rangle)}}}}. \tag{38}$$

The terminator $\mathcal{T}_{mi\nu\alpha}(\langle\boldsymbol{\xi}\rangle)$ may be approximated by that of the uniform medium

$$\mathcal{T}_{mi\nu\alpha}(\langle\boldsymbol{\xi}\rangle)\approx\mathcal{T}_{m\nu}=\cfrac{|\hat{b}_{m\nu}|^2}{\mathcal{L}_p^{-1}-\hat{a}_{m+1\nu}-\cfrac{|\hat{b}_{m+1\nu}|^2}{\cdots\cfrac{}{\cdots-\cfrac{|\hat{b}_{n-1\nu}|^2}{\mathcal{L}_p^{-1}-\hat{a}_{n\nu}-\mathcal{T}_{n\nu}}}}}. \tag{39}$$

Here, $\hat{a}_{l\nu}$ and $\hat{b}_{l\nu}$ are the recursion coefficients for the Hamiltonian $t_{i\nu j\nu'}\delta_{\sigma\sigma'}$. The last terminator $\mathcal{T}_{n\nu}$ with a large n may be replaced by

$$\mathcal{T}_{\infty\nu}=\frac{\mathcal{L}_p^{-1}-\hat{a}_{\infty\nu}-[(\mathcal{L}_p^{-1}-\hat{a}_{\infty\nu})^2-4|\hat{b}_{\infty\nu}|^2]^{1/2}}{2}. \tag{40}$$

The coefficients $\hat{a}_{\infty\nu}$ and $\hat{b}_{\infty\nu}$ are approximated by $\hat{a}_{\infty\nu}\approx(\hat{a}_{n-1\nu}+\hat{a}_{n\nu})/2$ and $|\hat{b}_{\infty\nu}|^2\approx(|\hat{b}_{n-1\nu}|^2+|\hat{b}_{n\nu}|^2)/2$.

In the present calculation scheme, we assume $[\langle\xi^2\rangle]_{\rm av}$ at low temperatures and obtain the uniform medium $\mathcal{L}_p^{-1}$ in the paramagnetic state. Under the uniform medium, we perform the MD calculations once according to Eqs. (10)~(12), and construct the initial set of $[\langle\xi^2\rangle]_{\rm av}$ and $\{\langle\boldsymbol{\xi}_j\rangle\}$ taking the time average. Then, we can construct the site-dependent effective medium (35): $\mathcal{L}_p^{-1}$ from $[\langle\xi^2\rangle]_{\rm av}$ and the site-dependent exchange potential $\tilde{J}_i\langle\boldsymbol{\xi}_i\rangle\cdot\boldsymbol{\sigma}/2$ from $\{\langle\boldsymbol{\xi}_j\rangle\}$. Using the site-dependent medium, we perform the full MD calculations and obtain a new set of $[\langle\xi^2\rangle]_{\rm av}$ and $\{\langle\boldsymbol{\xi}_j\rangle\}$. This procedure is repeated until the self-consistency is achieved. The LM's are finally calculated according to Eq. (9).

III. APPLICATION TO GAMMA MANGANESE

The MD approach presented in the last section takes into account the site-dependent molecular fields from the distant LM's in the ordered state. Therefore, it is expected that the theory describes more reasonably the cooperative phenomena such as the phase transition with increasing temperature. We applied the theory to γ-Mn to examine this feature. We adopted the Slater-Koster tight-binding parameters used by Pettifor,[23] the band width[25] 0.443 Ry, the d electron number $n=6.25$, and the effective exchange parameter[26] $\tilde{J}=0.060$ Ry. In the MD calculations, we used $N=108$ atoms (i.e., $3\times3\times3$ fcc lattice), and integrated Eqs. (10)~(12) up to a few thousand steps by means of the standard Runge-Kutta method with the time interval $\Delta t=0.04$ in unit of $T_{LM}=2\pi(2\mu_{LM}/\tilde{J})^{1/2}$, starting from a random configuration of $\{\boldsymbol{\xi}_j(t=0)\}$. In most cases, the selfconsistency of the site-dependent medium has been achieved after a few iterations.

Figure 2 shows the magnetic structure calculated at 25 K with use of the self-consistent site-dependent medium. The result shows the first-kind antiferromagnetic (AF) structure with the magnetic moment $|\langle\mathbf{m}_i\rangle|=2.50\mu_B$ in agreement with the experiment.[3,27] We verified that the selfconsistent MD calculations with use of $N=32$ atoms ($2\times2\times2$ fcc lattice) yield the same magnetic structure, so that the ambiguity due to system size is not important in the present case. When the temperature is increased, the fluctuations of the fictitious local moments become large, but their time developments are rather stable even near the Néel temperature T_N due to alternative molecular fields acting on each site as shown in Fig. 3.

We present in Fig. 4 the calculated local DOS with in-

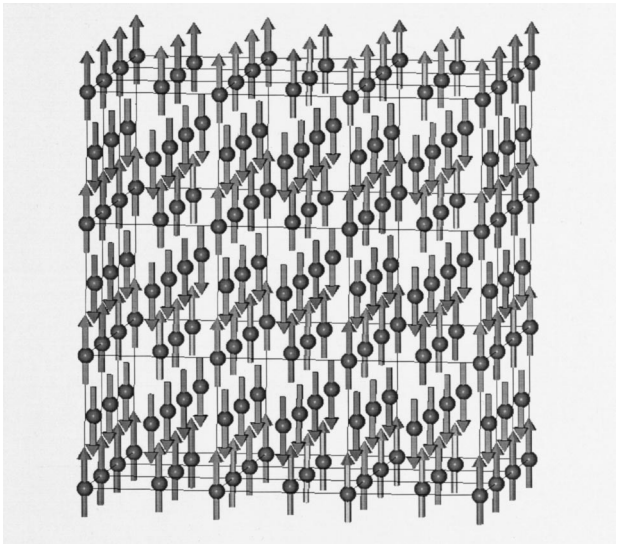

FIG. 2. The first-kind antiferromagnetic structure of γ-Mn at 25 K obtained by the MD approach with $N=108$ atoms and site-dependent selfconsistent medium.

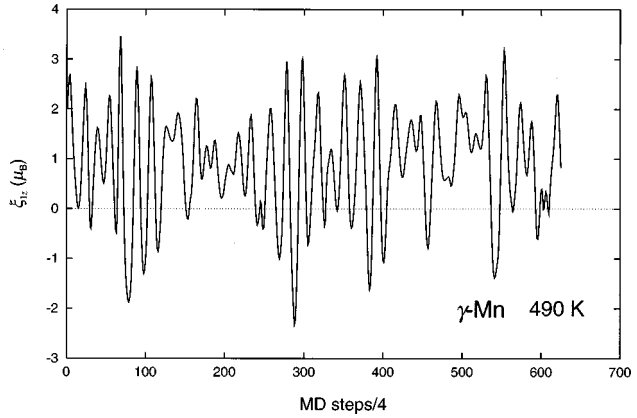

FIG. 3. The time development of a fictitious LM $\xi_{1z}(t)$ calculated near the Néel temperature T_N in the site-dependent self-consistent medium.

creasing temperatures, which are obtained from the formula.[28]

$$\rho_{i\sigma}(\omega)=\frac{(-)}{\pi}\,\mathrm{Im}\sum_{\nu}\,\langle G_{i\nu\sigma}(\omega+i\delta,\boldsymbol{\xi})\rangle. \tag{41}$$

Here, the thermal average $\langle\sim\rangle$ with respect to energy (5) was calculated by means of the time average. The up-spin DOS at low temperatures are characterized by two peaks around $\omega=-0.2$ Ry and smaller peaks around $\omega=0.1$ Ry, while the down-spin DOS consist of the large peak around $\omega=0.1$ Ry and a small peak around $\omega=-0.2$ Ry. A dip is therefore created near the Fermi level in the total DOS as shown in Fig. 5. This feature is consistent with the ground-state calculations and is considered to stabilize the first-kind AF structure.[7,12,29]

When we increase the temperature, the peaks around $\omega=-0.2$ Ry in the up-spin DOS become weaker and broader, while the small peaks around $\omega=0.1$ Ry develop rapidly and become a single peak. The main peak at $\omega=0.1$ Ry in the down-spin DOS, on the other hand, decreases rapidly with increasing thermal spin fluctuations, though it remains above T_N. It turns out that the dip near the Fermi level in the total DOS disappears above T_N as seen in Fig. 5. Moreover, the peak near the top of the *d* band remains above T_N in the total DOS. It should be noted that the DOS obtained by the conventional CPA does not show such a well-defined peak above T_N. This means that the peak in the DOS above T_N is created by the spin fluctuations with correlated motions.

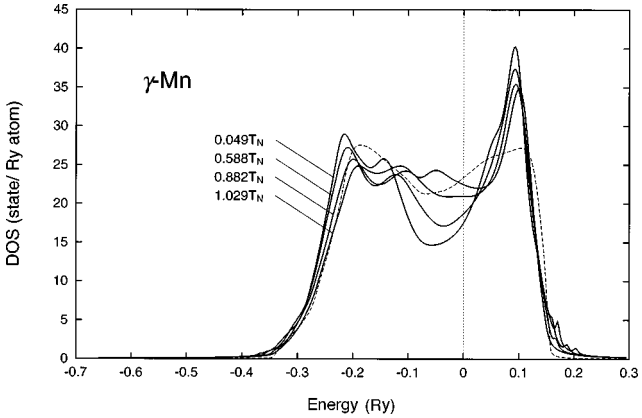

FIG. 5. Total DOS at various temperatures. Dashed curve is the DOS calculated by the conventional CPA at $1.029T_N$.

The temperature dependences of calculated magnetic moments are presented in Fig. 6. The amplitude of LM shows a weak temperature dependence; $\langle\mathbf{m}^2\rangle^{1/2}=3.77\mu_B$ at $T=0$ and $3.24\mu_B$ at $T=T_N$. On the other hand, the local magnetization smoothly decreases with increasing temperatures, revealing the second-order transition at $T_N=510$ K. Although the calculated Néel temperature agrees well with the experimental values (480~510 K), it seems to be accidental since the present approach treats the transverse spin fluctuations classically and the small number of atoms *N* in the MD unit cell tends to underestimate the magnetic entropy. We expect that calculated T_N would decrease by about 20% with increasing the system size *N*. This tendency is also found in the calculation of T_N by Ling *et al.*[30] who obtained $T_N=270$ K from the divergence of generalized susceptibility taking into account classical transverse spin fluctuations and the electronic structures calculated by the Koringer-Kohn-Rostoker (KKR)-CPA.

The MD approach allows us to calculate various physical quantities at finite temperatures. The magnetic short-range orders (MSRO), for example, are calculated from the formula.

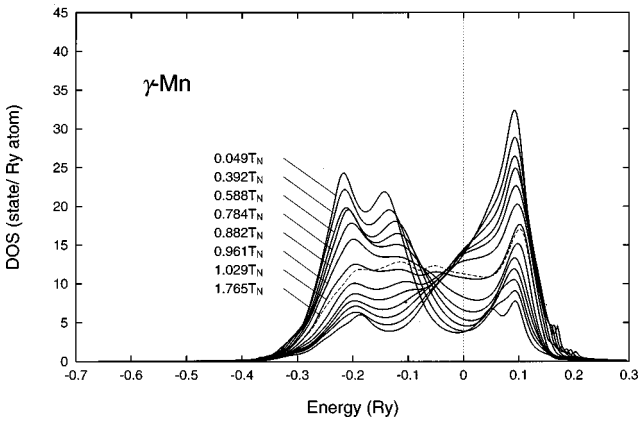

FIG. 4. Local densities of states (DOS) $\rho_{i\sigma}(\omega)$ for up and down spins at various temperatures.

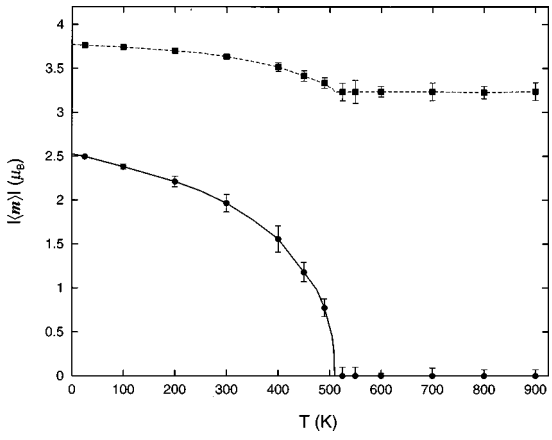

FIG. 6. Calculated temperature dependence of local magnetization $|\langle\mathbf{m}_i\rangle|$ (●) and the amplitude of LM $|\langle\mathbf{m}_i^2\rangle|^{1/2}$ (■) for γ-Mn.

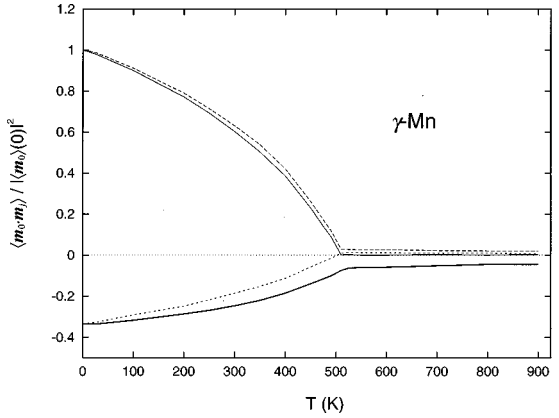

FIG. 7. Calculated magnetic short-range order $\langle \mathbf{m}_0 \cdot \mathbf{m}_j \rangle / |\langle \mathbf{m}_0 \rangle (T=0)|^2$ vs temperature curves for γ-Mn at first (thick line), second (dashed line), third (dotted line), and fourth (thin line) nearest-neighbor distances. Note that the curves below T_N are averaged over different magnetic sites.

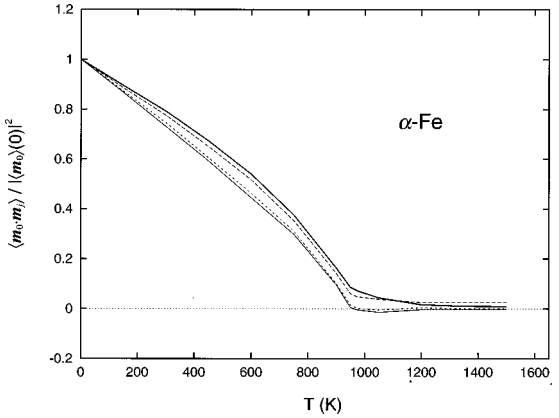

FIG. 8. Calculated magnetic short-range order vs temperature curves for α-Fe at first (thick line), second (dashed line), third (dotted line), and fourth (thin line) nearest-neighbor distances.

$$\langle \mathbf{m}_i \cdot \mathbf{m}_j \rangle = \left\langle \left(1 + \frac{4}{\beta \tilde{J}_i \xi_i^2} \right) \boldsymbol{\xi}_i \cdot \left(1 + \frac{4}{\beta \tilde{J}_j \xi_j^2} \right) \boldsymbol{\xi}_j \right\rangle . \quad (42)$$

Here, the thermal average $\langle \sim \rangle$ with respect to the energy (5) is calculated by the time average in the MD approach.

We present in Fig. 7 the MSRO defined by $\langle \mathbf{m}_0 \cdot \mathbf{m}_j \rangle / |\langle \mathbf{m}_0 \rangle (T=0)|^2$, which are calculated up to the fourth nearest-neighbor (NN) distance as a function of temperature. At the ground state, the NN MSRO on the ferromagnetic plane of the first-kind AF structure is 1, those between the NN ferromagnetic planes are -1 since the present theory is based on a classical approximation. The averaged value is therefore -0.333 as shown in Fig. 7. The second and fourth NN MSRO have no frustration, and therefore show the value 1 at the ground state. The third NN MSRO between the second NN ferromagnetic planes are 1 and other ones are -1, so that the average value becomes -0.333 at the ground state. With increasing temperature, all the MSRO monotonically decrease in magnitude, and show -0.074 at the NN distance, 0.030 at the second NN distance, 0.010 at the third NN distance, and 0.002 at the fourth NN distance at T_N. It should be noted that the MSRO for the third NN distance change the sign near T_N.

We calculated the MSRO of α-Fe with use of $N=128$ atoms to compare with those of γ-Mn. As shown in Fig. 8, the MSRO in α-Fe decrease from the value 1 at $T=0$ with increasing temperature, and have the values at T_C: 0.086 at the NN distance, 0.060 at the second NN distance, 0.010 at the third NN distance, and 0.00 at the fourth NN. The MSRO of γ-Mn at T_N are comparable to these values in magnitude. A remarkable difference between γ-Mn and α-Fe is that the first and third NN MSRO in γ-Mn show very weak temperature dependence above T_N as compared with those in α-Fe. In fact, the MSRO of γ-Mn calculated at $1.5T_N$ are -0.050 (first NN), 0.020 (second NN), and 0.010 (third NN), while those of α-Fe calculated at $1.5T_C$ are 0.010 (first NN), 0.025 (second NN), and 0.001 (third NN), respectively. Generally, the spin frustrations of LM's on the fcc lattice suppress the development of spin correlation with decreasing temperature. This is probably the reason for the weak temperature dependence in γ-Mn.

IV. SUMMARY

We have presented the MD approach to itinerant magnetism, which takes into account the molecular fields due to the distant LM's with complex magnetic structure by introducing the site-dependent noncollinear effective medium. Moreover, we derived an approximate form of the site-dependent medium expanding the local CPA equations from the paramagnetic state. The present approach allows us to investigate the temperature dependence of complex magnetic structures and related magnetic properties in itinerant electron systems by using the selfconsistent site-dependent medium.

We applied the theory to γ-Mn using $N=108$ atoms in the unit cell, and demonstrated that the theory can describe the second-order phase transition with increasing temperature. We obtained the first-kind AF structure with the Néel temperature $T_N=510$ K, which is consistent with the experimental data of γ-Mn, and weak temperature dependence of the amplitude of LM's.

The calculated MSRO at T_N show rather small values: -0.074 (first NN), 0.030 (second NN), and 0.010 (third NN). In particular, we found that the third NN MSRO changes the sign from the AF correlations to the ferromagnetic ones near T_N with increasing temperature, and that the first and third NN MSRO show a weak temperature dependence above T_N probably due to the strong spin frustrations. It is much desired to verify these behaviors on the MSRO by neutron experiments. Furthermore, we found considerable temperature dependence of the DOS; the dip of the DOS near the Fermi level disappears above T_N, while the main peak near the top of d band remains above T_N due to correlated spin fluctuations. These temperature dependences of DOS should be examined by the photoemission and inverse photoemission experiments in the future.

There are many other magnetic metals and alloys whose magnetic structures and magnetic properties have not yet been resolved in both experiment and theory. The magnetic structures of α-Mn, for example, have not been examined theoretically, though the structure was proposed by the neutron experiments[1] and was examined by the NMR experiments.[31] There is no direct experimental method to determine the magnetic structures of metallic surfaces and interfaces. It is desired to establish the theory of magnetic structure to these systems. Furthermore, one has to determine

both noncrystalline and magnetic structures in the theory of amorphous metallic magnetism.[32] We hope that further developments of the present approach will make it possible to determine and predict these magnetic structures and their magnetic properties quantitatively.

ACKNOWLEDGMENT

This work has been done partly with use of the facilities of the Supercomputer Center, Institute for Solid State Physics, University of Tokyo.

[1] T. Yamada, J. Phys. Soc. Jpn. **28**, 596 (1970); T. Yamada, N. Kunitomi, and Y. Nakai, *ibid.* **30**, 1614 (1971).
[2] Y. Tsunoda, J. Phys.: Condens. Matter **1**, 10 427 (1989).
[3] Y. Endoh and Y. Ishikawa, J. Phys. Soc. Jpn. **30**, 1614 (1971).
[4] S. Kawarazaki, K. Fujita, K. Yasuda, Y. Sasaki, T. Mizusaki, and A. Hirai, Phys. Rev. Lett. **61**, 471 (1988).
[5] K. Fukamichi, T. Goto, H. Komatsu, and H. Wakabayashi, in *Proceedings of the 4th International Conference on the Physics of Magnetic Materials, Poland, 1988*, edited by W. Gorkowski, H. K. Lachowics, and H. Szymczak (World Scientific, Singapore, 1989), p. 354.
[6] See, for example, Y. Kakehashi, S. Akbar, and N. Kimura, in *Itinerant Electron Magnetism: Fluctuation Effects & Critical Phenomena*, Vol. 55 of *NATO Science Series 3: High Technology*, edited by D. Wagner, W. Brauneck, and A. Sotontsov (Kluwer, Academic, Netherlands, 1998), pp. 193–228.
[7] S. Fujii, S. Ishida, and S. Asano, J. Phys. Soc. Jpn. **60**, 4300 (1991).
[8] C. Lacroix and C. Pinettes, J. Magn. Magn. Mater. **104–107**, 751 (1992).
[9] O. N. Mryasov, A. I. Lichtenstein, L. M. Sandratskii, and V. A. Gubanov, J. Phys.: Condens. Matter **3**, 7683 (1991); O. N. Mryasov, V. A. Gubanov, and A. I. Lichtenstein, J. Appl. Phys. **45**, 12 330 (1992).
[10] M. Uhl, L. M. Sandratskii, and J. Kübler, J. Magn. Magn. Mater. **103**, 314 (1992).
[11] M. Körling and J. Ergon, Phys. Rev. B **54**, 8293 (1996).
[12] S. Asano and J. Yamashita, J. Phys. Soc. Jpn. **31**, 1000 (1971).
[13] Y. Kakehashi, S. Akbar, and N. Kimura, Phys. Rev. B **57**, 8354 (1998).
[14] J. Hubbard, Phys. Rev. Lett. **3**, 77 (1959).
[15] R. L. Stratonovich, Dokl. Akad. Nauk SSSR **115**, 1097 (1958). [Sov. Phys. Dokl. **2**, 416 (1958)].
[16] Y. Kakehashi, Phys. Rev. B **34**, 3243 (1986).
[17] S. Nosé, J. Chem. Phys. **81**, 511 (1984).
[18] W. G. Hoover, *Computational Statistical Mechanics* (Elsevier, Amsterdam, 1991).
[19] S. Akbar, Y. Kakehashi, and N. Kimura, J. Phys.: Condens. Matter **10**, 2081 (1998).
[20] V. P. Antropov, S. V. Tretyakov, and B. N. Harmon, J. Appl. Phys. **81**, 3961 (1997).
[21] R. Haydock, V. Heine, and M. J. Kelly, J. Phys. C **8**, 591 (1975).
[22] V. Heine, R. Haydock, and M. J. Kelly, Solid State Phys. **35**, 1 (1980).
[23] R. Haydock and M. J. Kelly, Surf. Sci. **38**, 139 (1973).
[24] P. Soven, Phys. Rev. **156**, 809 (1967); B. Velický, S. Kirkpatrick, and H. Ehrenreich, *ibid.* **175**, 747 (1968).
[25] V. L. Moruzzi, J. F. Janak, and A. R. Williams, *Calculated Electronic Properties of Metals* (Pergamon, New York, 1978).
[26] J. F. Janak, Phys. Rev. B **16**, 255 (1977).
[27] D. Megeghetti and S. S. Sidhu, Phys. Rev. **105**, 130 (1957); G. E. Bacon, I. W. Dummur, J. H. Smith, and R. Street, Proc. R. Soc. London, Ser. A **241**, 223 (1957); T. J. Hick, A. R. Pepper, and J. H. Smith, J. Phys. C **1**, 1683 (1968).
[28] D. R. Hamann, Phys. Rev. B **2**, 1373 (1970).
[29] T. Oguchi and A. J. Freemann, J. Magn. Magn. Mater. **46**, L1 (1984).
[30] M. F. Ling, J. B. Staunton, D. D. Johnson, and F. J. Pinski, J. Magn. Magn. Mater. **177–181**, 1399 (1998).
[31] S. Murayama and H. Nagasawa, J. Phys. Soc. Jpn. **50**, 1189 (1981); **50**, 1523 (1981).
[32] J. A. Fernandez-Baca and W. Y. Ching, *The Magnetism of Amorphous Metals and Alloys* (World Scientific, Singapore, 1995).